A New Biosensor for Chiral Recognition Using Goat and Rabbit Serum Albumin Self-Assembled Quartz Crystal Microbalance

WEN-JING CHEN,[1] SHENG ZHANG,[2] WEI-GUANG ZHANG,[1]* JUN FAN,[1] XIA YIN,[1] SHENG-RUN ZHENG,[1] WEN-CUI SU,[1] ZHI ZHANG,[1] AND TAO HONG[1]

[1]*School of Chemistry and Environment, South China Normal University, Guangzhou, People's Republic of China*
[2]*Department of Chemistry, National University of Singapore, Singapore*

ABSTRACT Quartz crystal microbalance (QCM) biosensor was used for the chiral recognition of five pairs of enantiomers by using goat serum albumin (GSA) and rabbit serum albumin (RbSA) as chiral selectors. Serum albumin (SA) was immobilized on the QCM through the self-assembled monolayer technique, and the surface concentration of GSA and RbSA were 8.8×10^{-12} mol cm^{-2} and 1.2×10^{-11} mol cm^{-2}, respectively. The QCM biosensors showed excellent sensitivity and selectivity. Meanwhile, the chiral recognition of SA sensors was quite species dependent. There were differences between GSA and RbSA sensors in the ability and the preference of chiral recognition. To *R*,*S*-1,2,3,4-tetrahydro-1-naphthylamine (*R*,*S*-1-TNA), *R*,*S*-1-(4-methoxyphenyl)ethylamine (*R*,*S*-4-MPEA), and *R*,*S*-1-(3-methoxyphenyl)ethylamine (*R*,*S*-3-MPEA), the preference of the stereoselective SA-drug binding of the two kinds of SA sensors were consistent. However, to *R*,*S*-2-octanol (*R*, *S*-2-OT) and *R*,*S*-methyl lactate (*R*,*S*-MEL), the two kinds of SA sensors had opposite chiral recognition preference. Moreover, the interactions of SA and the five pairs of enantiomers have been further investigated through ultraviolet (UV) and fluorescent (FL) spectra. The UV/FL results were in accordance with the consequence of QCM. *Chirality 00:000–000, 2012.*

KEY WORDS: QCM; biosensor; serum albumin; chiral recognition; UV/FL spectra

INTRODUCTION

The detection of individual enantiomer remains an interesting and challenging task in analytical chemistry. It is well known that the molecules of different enantiomers can have significantly different pharmacological functions in living system, such as transport mechanism, toxicity, potency, and so on. Enantiomers have identical chemical and physical properties, and they only perform differently in a chiral environment. As a result, chiral recognition is challenging in chemistry, but nature offers an excellent alternative because chiral recognitions are fundamental phenomena in biological systems. Most biochemical processes routinely discriminate chiral molecules, such as drug distribution through the circulatory system by reversible binding to serum albumin (SA).[1] Accordingly, SAs have emerged as a class of ideal chiral selectors because they are one of the most abundant and extensively studied proteins in the circulatory system.[2] SAs have been widely applied to various chiral discrimination processes, such as high-performance liquid chromatography (HPLC), affinity ultrafiltration, affinity capillary electrophoresis, and thin-layer chromatography.[3–6] The degree and preference of stereoselective drug-binding processes are not necessarily constant among species. I. Fitos *et al.*[7] investigated stereoselective binding of benzodiazepine and coumarin drugs to SAs from human and six mammalian species by chiral chromatographic technique, and they found that the binding stereoselectivity of tofisopam in humans was opposite to that in all other species (dog, bovine, horse, pig, rabbit, and rat). A similar qualitative difference existed in the binding of *R*-warfarin and *S*-warfarin: human serum albumin (HSA) and rat serum albumin (RtSA) bind *S*-warfarin to a greater extent than *R*-warfarin, whereas rabbit serum albumin (RbSA) has the opposite enantioselectivity.[1,8] Arai *et al.*[9] applied capillary affinity zone electrophoresis to investigate the enantioselective ofloxacin—albumin binding and the results showed that albumins from different species (rabbit, goat, dog, bovine, horse, egg, and guinea pig) possessed different chiral separation abilities. Because animal models are usually used in protein binding, pharmacokinetic and pharmacodynamic studies, the conclusions derived from these studies are often extrapolated to humans. It is important to identify interspecies differences in the enantioselectivity of the protein-binding process.

Chromatographic techniques such as HPLC, gas chromatography, and capillary electrophoresis with chiral stationary phases (CSPs) have been well developed in enantioseparation of chiral isomers over the past decades.[10,11] They exhibit some advantages, such as high efficiency, easy standardization, and widespread use. However, some drawbacks such as expensive CSPs, laborious and time-consuming operations, have been shown in practical studies. In comparison with those traditional methods, quartz crystal microbalance (QCM) sensors for enantiomers recognition and determination have been testified in the literatures previously reported, as much more mass sensitivity, rapider analysis speed, lower cost, more suitable for real-time analysis as well as potential

Additional Supporting Information may be found in the online version of this article.
Contract grant sponsor: Natural Science Foundation of China (NSFC); Contract grant numbers: NSFC-21171059.NSFC-21003053.
Contract grant sponsor: Guangdong Science and Technology Department (GDST).; Contract grant numbers: GDST- 2010B050300021.GDST-2011B010400023.
*Correspondence to: W-G. Zhang, School of Chemistry and Environment, South China Normal University, Guangzhou 510006, People's Republic of China. E-mail: wgzhang@scnu.edu.cn
Received for publication 05 February 2012; Accepted 13 April 2012
DOI: 10.1002/chir.22074
Published online in Wiley Online Library (wileyonlinelibrary.com).

lab-on-a-chip use.[12–18] Toyo'oka *et al.*[14] firstly developed QCM sensors immobilized with CSP materials as a simple, rapid, and effective screening method to predict separation efficiency of pairs of enantiomers during chiral HPLC. Guo *et al.*[15] used QCM technique to predict the chiral recognizability of a chiral selector (L-phenylalanine) for L-mandelic and D-mandelic acid. Ng *et al.*[16] have demonstrated 10 chiral sensors immobilized with mercaptyl perfunctionalized β-cyclodextrins, which exhibited the promising enantioselectivity to three pairs of enantiomers (*R*,*S*-methyl lactate, *R*,*S*-ethyl lactate, and *R*,*S*-2-octanol) in the gas phase. Chan *et al.*[17] have reported enantioselective molecular imprinting polymer-coated QCM for the recognition of L-tryptophan. Cheng *et al.*[18] designed and synthesized three chiral bicyclodipeptide-bearing calix[4]arenes for application in gas QCM sensors, and all of these compounds exhibited significant chiral discrimination for the enantiomers of methyl lactate.

The key step for selectively sensing chiral compounds using a QCM sensor is to build a chiral surface with recognition sites for the enantiomers. Self-assembled monolayers (SAMs) of thiolates often constitute a base layer of thiolates with free carboxylic acids as terminal groups. Carboxylic acid can be activated by 1-ethyl-3-(3-dimethylaminopropyl) carbodiimide (EDC) and *N*-hydroxysuccinimide (NHS) for protein binding. By this method, proteins can be chemically bound with controlled order and density on the gold surface. Because SAs are biological macromolecules, their native structures should be carefully preserved during immobilization to maintain their functionality.[19–22] Researchers have used SAM techniques to successfully fabricate various QCM biosensors, which exhibited excellent response and bioactivity.[23–26] Herein, SAM was selected as the immobilization method to anchor proteins.

In our previous work, we developed a class of QCM chiral sensors with self-assembled bovine serum albumin (BSA) or HSA for real-time chiral recognition, and these biosensors got promising selectivity.[27] Regarding the aspect of species dependency in chiral-drug recognition of SAs, a series of new chiral biosensors with self-assembled RbSA and goat serum albumin (GSA) were fabricated for real-time chiral recognition in this work. In addition, the interactions of SA and the enantiomers have been further investigated through ultraviolet (UV) and fluorescent (FL) spectra.

EXPERIMENTAL

Materials

The structures of five pairs of enantiomers obtained from Alfa Aesar (Tianjin, China) are shown in Scheme 1. Both GSA and RbSA were purchased from BaiTai Ke Biotechnology Co., Ltd (Luoyang, China). The solutions of GSA and RbSA were freshly prepared in the buffer (0.05 mol l^{-1} Tris–HCl and 0.1 mol l^{-1} NaCl, pH 7.4) and diluted to the experimental concentration. All other chemicals were of analytical grade. Deionized water (Aquapro, ARU-L-500L) was used throughout the current research.

Quartz Crystal Microbalance System

The QCM measurements in gas phase were carried out using AT-cut, 8-MHz quartz piezoelectric crystals (Chenhua Co., Ltd, Shanghai, China) (1.2-cm diameter, 0.5-mm thickness, and gold plated on both faces). The QCM measurements in liquid phase were carried out using AT-cut quartz crystals coated with gold (fundamental frequency of 5 MHz, Q-Sense AB, Sweden). The immobilization processes of SAs on QCM crystals were measured by a home-made flow injection analysis (FIA) system, which was similar to that used in the reported literature.[28] Chiral discrimination was investigated by using a home-made QCM gas system described previously.[27,29]

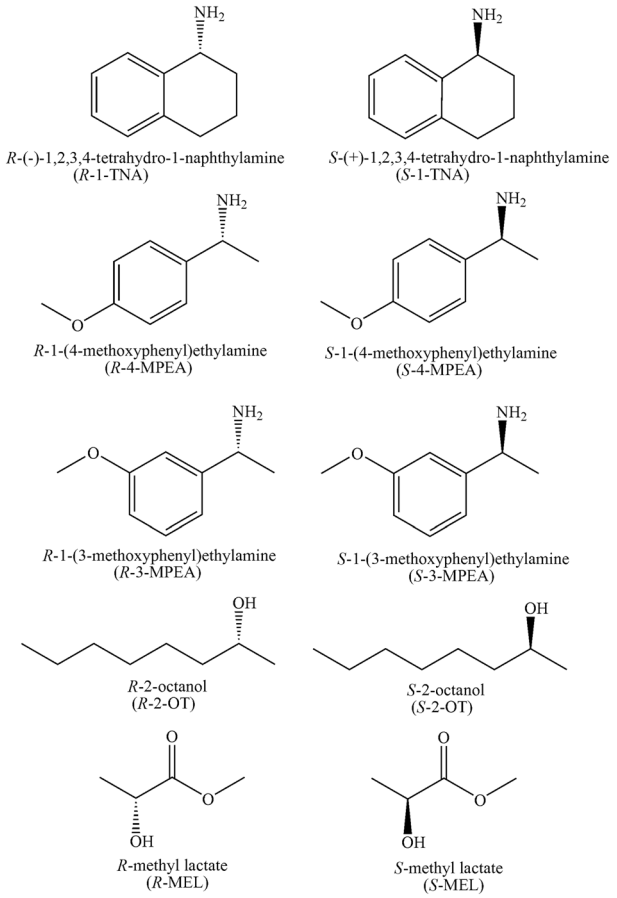

Scheme 1. The structures of five pairs of enantiomers.

The Fabrication Procedure of Serum Albumin Self-Assembled Quartz Crystal Microbalance Biosensor

The SA quartz crystal sensors were prepared by using a three-step assembling process. The QCM crystal was cleaned with piranha solution (98% H_2SO_4 : 30% H_2O_2 (v/v) 7:3) for 5–10 min and thoroughly rinsed with deionized water and ethanol, followed by drying with N_2. Subsequently, QCM crystal was immersed in 1 mmol l^{-1} of mercaptoacetic acid in ethanol for 24 h at room temperature to form a SAM. Then, the SAM was activated with 2 mmol l^{-1} of EDC and 5 mmol l^{-1} of NHS in mixed aqueous solution for 3 h.

The third step of self-assembly process was monitored using QCM integrated with the FIA system. The EDC-NHS-activated quartz crystal was mounted in the FIA system and rinsed with 0.05 mol l^{-1} of Tris–HCl (0.1 mol l^{-1} of NaCl, pH 7.4) continuously until the frequency reached stabilization under the flow conditions (20 μl min^{-1}). The solvent was then changed to 1.5×10^{-5} mol l^{-1} of GSA or RbSA in Tris–HCl solution. The frequency shifts were recorded versus time.

Chiral Recognition of Five Pairs of Enantiomers by Quartz Crystal Microbalance Biosensor

The SA-fabricated QCM biosensors were mounted in the gas phase pulse-measuring system,[27,29] a vaporization pad that allowed microscale enantiomeric samples to be evaporated. Predried pure nitrogen was used as carrier gas. The gas flow rate was controlled at 250 ± 2 ml min^{-1} by an Alicat mass flow meter. Sample injection volume was 4.0 μl.

Ultraviolet and Fluorescent Spectra

For UV and FL spectra, a 1.0×10^{-5} mol l^{-1} of SA in Tris–HCl buffer (2.0 ml) was added accurately into a 1.0-cm quartz cell and then titrated by successive additions of 1.0×10^{-2} mol l^{-1} each single enantiomer to

attain a series of concentrations gradient. The UV absorption measurements in the range from 240 to 320 nm were performed on a UV-1700 spectrophotometer (Shimadzu, Japan) at room temperature. Fluorescence spectra were recorded on an FLS-920 spectrophotometer (Edinburgh, England) from 285 to 450 nm at room temperature.

RESULTS AND DISCUSSION

Real-Time Monitor of the Self-Assembly Process of Immobilization Serum Albumin to the Activated Quartz Crystal Microbalance Surface

Quartz crystal microbalance integrated in an FIA system has the advantage to work continuously and to monitor online binding of the analyte; hence, a highly automated performance can be achieved.[28] FIA system was used to monitor the third step of self-assembly. As shown in Figure 1, the frequency gradually decreased when 1.5×10^{-5} mol l^{-1} of GSA or RbSA in Tris–HCl solution was flowed over the activated QCM surface. The frequency shift indicated the mass increase of SA on the activated QCM surface. After about 5–6 h, a plateau was reached. Δf_{GSA} (−33 Hz) was lower than Δf_{RbSA} (−45 Hz), indicating stronger adsorption of RbSA. The SA functionalized QCM surface was a monolayer and rigid deposition, so the surface concentration (Θ) of SA can be calculated using Equation (1):[26,27]

$$\Theta = -C\frac{\Delta f}{M} \quad (1)$$

where C is the mass sensitivity constant ($C = 17.7$ ng cm^{-2} Hz^{-1} for a 5-MHz crystal [22]), M is the molecular weight of chiral selector (for GSA, $M = 66{,}300$ Da; for RbSA, $M = 66{,}150$ Da[30]).

On the basis of Equation 1, the surface concentrations of immobilized GSA and RbSA were 8.8×10^{-12} mol cm^{-2} and 1.2×10^{-11} mol cm^{-2}, respectively.

Real-Time Chiral Recognition of Enantiomers by Goat Serum Albumin and Rabbit Serum Albumin Sensors

The frequency changes were measured against time as each single enantiomer was injected into the gas system to interact with GSA or RbSA. The decreased frequency indicated interactions between enantiomers and SA, and the results could reproduce over five consecutive measurements. Frequency shifts were the same when individual *R*-enantiomers or *S*-enantiomers were introduced onto the blank sensor, implying no enantioselectivity. The interactions of five pairs of enantiomers on GSA-modified and RbSA-modified QCM biosensors are shown in Figs. S1 and S2 (Supporting Information). The binding affinities of GSA and RbSA for five pairs of enantiomers were enantioselective. In addition, the frequency shifts were significantly different in response to the absorption of enantiomers on both GSA and RbSA sensors.

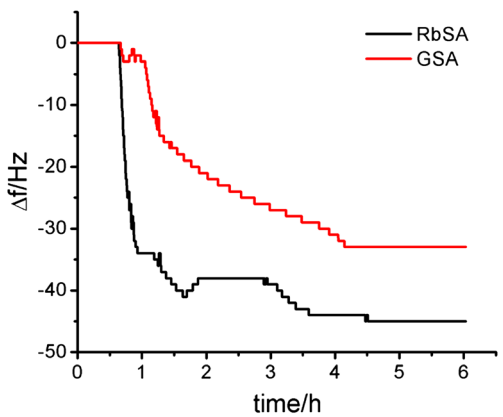

Fig. 1. Immobilization of goat serum albumin (GSA) and rabbit serum albumin (RbSA) to the activated quartz crystal microbalance surface.

The QCM chiral discrimination factor α_{QCM} of five pairs of enantiomers for both the GSA and RbSA sensors were calculated according to Equation (2):[27,29]

$$\alpha_{QCM} = \frac{\Delta f_R}{\Delta f_s} \text{ or } \alpha_{QCM} = \frac{\Delta f_s}{\Delta f_R} \quad (2)$$

For GSA sensor, the α_{QCM} can be ranked in decreasing order: *R*,*S*-1,2,3,4-tetrahydro-1-naphthylamine (*R*,*S*-1-TNA; $\alpha_{QCM} = 1.34$) > *R*,*S*-1-(4-methoxyphenyl)ethylamine (*R*,*S*-4-MPEA; $\alpha_{QCM} = 1.22$) > *R*,*S*-methyl lactate (*R*,*S*-MEL; $\alpha_{QCM} = 1.16$) > *R*,*S*-2-octanol (*R*,*S*-2-OT; $\alpha_{QCM} = 1.12$) > *R*,*S*-1-(3-methoxyphenyl)ethylamine (*R*,*S*-3-MPEA; $\alpha_{QCM} = 1.06$). Similarly, the α_{QCM} of RbSA sensor can be ranked in decreasing order: *R*,*S*-1-TNA ($\alpha_{QCM} = 1.28$) > *R*,*S*-4-MPEA ($\alpha_{QCM} = 1.19$) > *R*,*S*-2-OT ($\alpha_{QCM} = 1.14$) > *R*,*S*-MEL ($\alpha_{QCM} = 1.11$) = *R*,*S*-3-MPEA ($\alpha_{QCM} = 1.11$). *R*,*S*-1-TNA, *R*,*S*-4-MPEA, and *R*,*S*-MEL were more easily recognized by the GSA sensor compared with the RbSA sensor. In addition, the RbSA sensor showed slightly higher chiral discrimination for *R*,*S*-3-MPEA and *R*,*S*-2-OT than GSA sensor (Fig. S3, Supporting Information).

Chiral discrimination factor (α_{QCM}) can't be normalized to the surface concentration of immobilized SA molecules (the surface concentration of RbSA sensor was higher than the GSA sensor). The selectivity of the sensor was affected significantly by both the surface concentration and the nature of chiral selectors (GSA and RbSA). Although SAs of different species have similar structures with 70–80% identical amino acid sequence,[2] RbSA and GSA show different chiral recognition abilities, which are similar to the literatures reported previously.[7–9]

Comparison of the Discriminating Abilities of Serum Albumin from Different Species

Chiral discriminating abilities of four SA chiral sensors (BSA[27], HSA[27], RbSA, and GSA) were listed in Table 1. *S*-enantiomer of 1-TNA was always better bound as indicated by the higher frequency shifts than the *R*-enantiomer ($S > R$), whereas *R*-enantiomer of 4-MPEA always showed stronger binding than *S*-enantiomer ($R > S$). On the other hand, the other three pairs of enantiomers exhibited opposite stereoselectivities for the SA of different species. In case of *R*,*S*-3-MPEA, *R*-3-MPEA was preferred to *S*-3-MPEA for all species except for HSA, which exhibited opposite enantioselectivity ($S > R$). To *R*,*S*-2-OT and *R*,*S*-MEL, RbSA chiral sensor showed its special enantioselectivity, RbSA bound *S*-2-OT and *S*-MEL slightly stronger than *R*-2-OT and *R*-MEL, whereas the three other SA sensors (BSA, GSA, and HSA) have the opposite enantioselectivity ($R > S$).

Serum albumins of different species have very similar structures, with 70–80% identical amino acid sequence.[2] However, the degree and preference of the stereoselective drug-binding process are not necessarily constant among species. Similar phenomena were also found in other drug-SA binding.[7–9] Our results, as well as those published in the literatures, might reflect a species specific sequence of the amino acids and conformation, which constitute the specific binding sites for 3-MPEA, 2-OT, and MEL, whereas the

TABLE 1. The α_{QCM} of four serum albumin sensors

Species	QCM chiral discrimination factor α_{QCM}				
	1-TNA	4-MPEA	3-MPEA	2-OT	MEL
Goat (GSA)	1.34 ($S > R$)	1.22 ($R > S$)	1.06 ($R > S$)	1.12 ($R > S$)	1.16 ($R > S$)
Rabbit (RbSA)	1.28 ($S > R$)	1.19 ($R > S$)	1.11 ($R > S$)	1.14 ($S > R$)	1.11 ($S > R$)
Human (HSA)	1.57 ($S > R$)	1.18 ($R > S$)	1.06 ($S > R$)	1.16 ($R > S$)	1.13 ($R > S$)
Bovine (BSA)	1.34 ($S > R$)	1.20 ($R > S$)	1.16 ($R > S$)	1.15 ($R > S$)	1.11 ($R > S$)

The value of HSA and BSA are from our previous work.[27]
QCM, quartz crystal microbalance; GSA, goat serum albumin; RbSA, rabbit serum albumin; HSA, human serum albumin; BSA, bovine serum albumin.

sequence of the binding sites of 1-TNA and 4-MPEA were less variable among species.

Investigation of the Interaction Between Serum Albumin and Enantiomers by Ultraviolet Spectra

Goat serum albumin has an absorption maximum of 280 nm, which can be assigned to the aromatic heterocyclic hydrophobic groups of Trp residues and Tyr residues.[31] Hence, UV spectra of the samples in the range of 240–320 nm were recorded (Fig S4, Supporting Information). With the addition of the single enantiomer of *R/S*-1-TNA, *R/S*-3-MPEA, and *R/S*-4-MPEA to GSA solution, the characteristic absorption peak of GSA at 280 nm gradually increased in intensity with a slight blue shift. Addition of 1-TNA, 4-MPEA, and 3-MPEA may induce the peptide chain of SA to stretch and the aromatic heterocyclic hydrophobic groups of Trp residues and Tyr residues to be exposed. At the same time, hydrophobic interaction was weakened, and the energy of $n \rightarrow \pi^*$ and $\pi \rightarrow \pi^*$ transition was increased, which resulted in a slight blue shift when the complex was formed.[27] After adding *R*-2-OT or *S*-2-OT and *R*-MEL or *S*-MEL, the peak at 280 nm decreased without any shift in wavelength. It may be explained that the hydroxyl groups (−OH) in 2-OT and MEL form typical hydrogen bonds with the amino acid residues of SA molecules, and some covalent bonds in SA molecules would be weakened.[27] In addition, the absorption intensities of the two spectra between *R*-enantiomers and *S*-enantiomers were different, indicating their different interactions with GSA. Similar UV spectra of RbSA with five pairs of enantiomers can be found in Fig. S5 (Supporting Information).

Ultraviolet binding constant (K_A) was calculated according to the modified Hildebrand–Benesi Equation (3): [32,33]

$$\frac{1}{A_0 - A} = \frac{1}{K_A} \cdot \frac{1}{C} + I \tag{3}$$

where K_A is the binding constant, C is the concentration of enantiomer, $A_0 - A$ is the change of absorption intensity of SA by addition of single enantiomer. There were good linear relationships between $1/(A_0 - A)$ and $1/C$, and all the regression coefficient (R^*) were larger than 0.99 indicating the 1:1 complex conformation. The larger binding constant K_A means more stable complex formed between SA and single enantiomer. The chiral recognition factor (α_{UV}) was determined using Equation (4): [27,29]

$$\alpha_{UV} = 2\frac{|\lg K_R - \lg K_S|}{\lg K_R + \lg K_S} \tag{4}$$

All the binding constants (K_A) and UV chiral discrimination factors (α_{UV}) were shown in Table 2. In comparison with the QCM results, the similar UV chiral discrimination trend was found.

Investigation of the Interaction Between Serum Albumin and Enantiomers by Fluorescent Spectra

Goat serum albumin emits strong intrinsic fluorescence at 332 nm when excited at 280 nm. The fluorescence intensity of GSA was obviously weakened with increase of the concentration of 10 single enantiomers (Fig. S6, Supporting Information). The possible factors of fluorescence quenching were the alteration of GSA conformation and the change of the microenvironment because of bind of *R*-enantiomers or *S*-enantiomers. FL spectra of RbSA with five pairs of enantiomers can be found in Fig. S7 (Supporting Information). When experimental conditions such as pH value (Tris–HCl, pH 7.4),

TABLE 2. The ultraviolet binding constants (K_A) and ultraviolet chiral discriminition factors (α_{UV})

Enantiomers	Binding constants K_A				α_{UV}	
	GSA	R*	RbSA	R*	GSA	RbSA
R-1-TNA	104.3	0.9928	84.4	0.9952	0.355	0.319
S-1-TNA	775.2	0.9922	454.5	0.9938		
R-4-MPEA	1995.0	0.9922	1831.7	0.9939	0.244	0.128
S-4-MPEA	383.1	0.9951	740.7	0.9906		
R-3-MPEA	1486.2	0.9999	1559.4	0.9999	0.016	0.024
S-3-MPEA	1326.3	0.9999	1312.3	0.9983		
R-2-OT	48.4	0.9987	41.6	0.9980	0.074	0.093
S-2-OT	36.7	0.9995	59.8	0.9996		
R-MEL	54.5	0.9924	42.3	0.9987	0.101	0.048
S-MEL	37.2	0.9999	50.8	0.9990		

GSA, goat serum albumin; RbSA, rabbit serum albumin.

TABLE 3. All the fluorescent binding constants (K_a) and fluorescent chiral discrimination factors (α_{FL})

Enantiomers	Binding constants K_a				α_{FL}	
	GSA	R*	RbSA	R*	GSA	RbSA
R-1-TNA	81.3	0.9917	81.1	0.9959	0.330	0.291
S-1-TNA	461.4	0.9919	364.1	0.9928		
R-4-MPEA	1149.4	0.9955	1846.5	0.9914	0.266	0.153
S-4-MPEA	219.3	0.9967	635.3	0.9949		
R-3-MPEA	2091.5	0.9975	92072.5	0.9976	0.029	0.042
S-3-MPEA	1670.0	0.9916	57619.5	0.9960		
R-2-OT	703.1	0.9965	498.1	0.9926	0.095	0.137
S-2-0T	387.0	0.9978	1241.8	0.9951		
R-MEL	213.5	0.9904	234.6	0.9989	0.136	0.053
S-MEL	107.7	0.9911	319.9	0.9933		

GSA, goat serum albumin; RbSA, rabbit serum albumin.

temperature, and ionic strength were fixed, fluorescence quenching may result from ground complex formation, energy transfer, and dynamic quenching processes. The dynamic quenching is caused by the collision between FL molecules and quenchers, whereas static quenching is due to formation of nonfluorescent complexes through the reaction of FL molecules and quenchers. To shed light on the fluorescence quenching mechanism, fluorescence quenching data are analyzed by the Stern–Volmer equation[34], and quenching rate constants (Kq) for GSA and RbSA were listed in Table S1 (Supporting Information). All the Kq data were larger than the maximum value of collision quenching constant (2.0×10^{10}1 $mol^{-1}\,s^{-1}$), which confirmed that the SA quenching processes were caused by static quenching mechanisms.[35] Thus, association constant (K_a) and the number of binding sites (n) can be obtained from the double-logarithm curve on the basis of the static quenching Equation (5):[36]

$$\lg\frac{F_0 - F}{F} = \lg K_a + n\lg[Q] \quad (5)$$

where F_0 and F are the fluorescence intensity before and after addition of single enantiomer, respectively, and $[Q]$ is the concentration of single enantiomer.

Fluorescence chiral recognition factor (α_{FL}) is defined in the same manner as UV discrimination factor (α_{UV}). The binding constants (K_a) and FL chiral discrimination factors (α_{FL}) are shown in Table 3. For each pair of enantiomers, QCM chiral discrimination factors (α_{QCM}), UV discrimination factors (α_{UV}), and fluorescence discrimination factors (α_{FL}) were consistent (Table 4), which indicated that these SA-modified QCM chiral biosensors were sensitive and selective enough to recognize enantiomers. It might become a simple, rapid, and real-time chiral recognition method in the future.

TABLE 4. Comparison of chiral discrimination factors from quartz crystal microbalance, ultraviolet, and fluorescent techniques

Enantiomer	GSA			RbSA		
	α_{QCM}	α_{UV}	α_{FL}	α_{QCM}	α_{UV}	α_{FL}
R,*S*-1-TNA	1.34	0.355	0.330	1.28	0.319	0.291
	$S > R$	$S > R$	$S > R$	$S > R$	$S > R$	$S > R$
R,*S*-4-MEPA	1.22	0.244	0.266	1.19	0.128	0.153
	$R > S$	$R > S$	$R > S$	$R > S$	$R > S$	$R > S$
R,*S*-3-MPEA	1.06	0.016	0.029	1.11	0.024	0.042
	$R > S$	$R > S$	$R > S$	$R > S$	$R > S$	$R > S$
R,*S*-2-OT	1.12	0.074	0.095	1.14	0.093	0.137
	$R > S$	$R > S$	$R > S$	$S > R$	$S > R$	$S > R$
R,*S*-MEL	1.16	0.101	0.136	1.11	0.048	0.053
	$R > S$	$R > S$	$R > S$	$S > R$	$S > R$	$S > R$

GSA, goat serum albumin; RbSA, rabbit serum albumin.

CONCLUSIONS

A series of QCM chiral biosensors were obtained through SAM of SA (GSA or RbSA). The processes of the immobilization of SA to the activated QCM sensors were real-time monitored using QCM integrated with FIA. The surface concentrations of GSA and RbSA immobilized on gold surface were 8.8×10^{-12} mol cm^{-2} and 1.2×10^{-11} mol cm^{-2}, respectively. These SA QCM chiral sensors exhibited excellent sensitivity and enantioselectivity to five pairs of enantiomers. However, the chiral discrimination of SA sensors was species dependent. There were differences between GSA and RbSA sensors in chiral recognition degree and preference. For GSA sensor, the maximum α_{QCM} value was 1.34 (*R*,*S*-1-TNA) and the minimum was 1.06 (*R*,*S*-3-MEPA), whereas for RbSA sensor, the highest and lowest chiral discrimination factors were 1.28 (*R*,*S*-1-TNA) and 1.11 (*R*,*S*-3-MPEA and *R*,*S*-MEL), respectively. Meanwhile, to *R*,*S*-2-OT and *R*,*S*-MEL, opposite chiral recognition preference was observed on two SA sensors. Moreover, the UV and FL spectra have been used to investigate the interactions between SA and enantiomers. The chiral recognition trend based on QCM, UV, and FL techniques were consistent. Because the investigation of chiral recognition was carried out in gas phase in this work, samples were limited to the enantiomers, which can easily evaporate. Further studies will focus on chiral recognition by QCM technique in liquid phase.

LITERATURE CITED

1. Massolini G, Aubry AF, McGann A, Wainer IW. Determination of the magnitude and enantioselectivity of ligand binding to rat and rabbit serum albumins using immobilized-protein high performance liquid chromatography stationary phases. Biochem Pharmacol 1993;46:1285–1293.
2. Peters T. *All about albumin*. New York: Academic Press; 1996.
3. Zhai Z, Chen Y, Wang YJ, Luo GS. Chiral separation performance of micrometer-sized monodispersed silica spheres with high protein loading. Chirality 2009;21:760–768.

4. Edwie F, Li Y, Chung TS. Exploration of regeneration and reusability of human serum albumin as a stereoselective ligand for chiral separation in affinity ultrafiltration. J Membr Sci 2010;362:501–508.
5. Ye H, Yu L, Xu X, Zheng C, Lin W, Liu X, Chen G. Affinity capillary electrophoresis coupling with partial filling technique and field-amplified sample injection for enantioseparation and determination of DL-tetrahydropalmatine. Electrophoresis 2010;31:2049–2054.
6. Lepri L, Coas V, Desideri P, Santianni D. Reversed phase planar chromatography of dansyl DL amino acids with bovine serum albumin in the mobile phase. Chromatographia 1993;36:297–301.
7. Fitos I, Visy J, Simonyi M. Species-dependency in chiral-drug recognition of serum albumin studied by chromatographic methods. J Biochem Bioph Methods 2002;54:71–84.
8. Lagercrantz C, Larsson T, Denfors I. Stereoselective binding of the enantiomers of warfarin and trytophan to serum albumin from some different species studied by affinity chromatography on columns of immobilized serum albumin. Comp Biochem Phys C 1981;69:375–378.
9. Arai T, Nimura N, Kinoshita T. Investigation of enantioselective ofloxacin-albumin binding and displacement interactions using capillary affinity zone electrophoresis. Biomed Chromatogr 1995;9:68–74.
10. Ahuja S. *Chiral separations by chromatography*. Washington D C: Oxford University Press; 2000.
11. Ward TJ. Chiral separations. Anal Chem 2006;78:3947–3956.
12. Inomata T, Eguchi H, Matsumoto K, Funahashi Y, Ozawa T, Masuda H. Adsorption of microorganisms onto an artificial siderophore-modified Au substrate. Biosens Bioelectron 2007;23:751–755.
13. Ng SC, Sun T, Chan HSO. Durable chiral sensor based on quartz crystal microbalance using self-assembled monolayer of permethylated β-cyclodextrin. Macromol Symp 2003;192:171–181.
14. Inagaki S, Min JZ, Toyo'oka T. Prediction for the separation efficiency of a pair of enantiomers during chiral high-performance liquid chromatography using a quartz crystal microbalance. Anal Chem 2008;80:1824 – 1828.
15. Guo HS, Kim JM, Pham XH, Chang SM, Kim WS. Predicting the enantioseparation efficiency of chiral mandelic acid in diastereomeric crystallization using a quartz crystal microbalance. Cryst Growth Des 2011;11:53–58.
16. Xu CH, Ng SC, Chan HSO. Self-assembly of perfunctionalized β-cyclodextrins on a quartz crystal microbalance for real-time chiral recognition. Langmuir 2008;24:9118–9124.
17. Liu F, Liu X, Ng SC, Chan HSO. Enantioselective molecular imprinting polymer coated QCM for the recognition of L-tryptophan. Sens Actuators B 2006;113:234–240.
18. Guo W, Wang J, Wang C, He JQ, He XW, Cheng JP. Design, synthesis, and enantiomeric recognition of dicyclodipeptide-bearing calix[4]arenes: a promising family for chiral gas sensor coatings. Tetrahedron Lett 2002;43:5665–5667.
19. Briand E, Gu C, Boujday S, Salmain M, Herry JM, Pradier CM. Functionalisation of gold surfaces with thiolate SAMs: topography/bioactivity relationship – a combined FT-RAIRS, AFM and QCM investigation. Surf Sci 2007;601:3850–3855.
20. Ignat T, Miu M, Kleps I, Bragaru A, Simion M, Danila M. Electrochemical characterization of BSA/11-mercaptoundecanoic acid on Au electrode. Mater Sci Eng B 2010;169:55–61.
21. Chen JC, Sadhasivam S, Lin FH. Label free gravimetric detection of epidermal growth factor receptor by antibody immobilization on quartz crystal microbalance. Process Biochem 2011;46:543–550.
22. Hong SR, Choi SJ, Jeong HD, Hong S. Development of QCM biosensor to detect a marine derived pathogenic bacteria Edwardsiella tarda using a novel immobilisation method. Biosens Bioelectron 2009;24:1635–1640.
23. Buchatip S, Ananthanawat C, Sithigorngul P, Sangvanich P, Rengpipat S, Hoven VP. Detection of the shrimp pathogenic bacteria, Vibrio harveyi, by a quartz crystal microbalance-specific antibody based sensor. Sens Actuators B 2010;145:259–264.
24. Hao RZ, Wang DB, Zhang XE, Zuo GM, Wei HP, Yang RF, Zhang ZP, Cheng ZX, Guo YC, Cui ZQ, and others. Rapid detection of Bacillus anthracis using monoclonal antibody functionalized QCM sensor. Biosens Bioelectron 2009;24:1330–1335.
25. Liu YC, Wang CM, Hsiung KP. Comparison of different protein immobilization methods on quartz crystal microbalance surface in flow injection immunoassay. Anal Biochem 2001;299:130–135.
26. Wang XY, Ruengruglikit C, Wang YW, Huang QR. Interfacial interactions of pectin with bovine serum albumin studied by quartz crystal microbalance with dissipation monitoring: effect of ionic strength. J Agric Food Chem 2007;55:10425–10431.
27. Su WC, Zhang WG, Zhang S, Fan J, Yin X, Luo ML, Ng SC. A novel strategy for rapid real-time chiral discrimination of enantiomers using serum albumin functionalized QCM biosensor. Biosens Bioelectron 2009;25:488–492.
28. Liu Y, Yu X, Zhao R, Shangguan DH, Bo Z, Liu G. Quartz crystal biosensor for real-time monitoring of molecular recognition between protein and small molecular medicinal agents. Biosens Bioelectron 2003;19:9–19.
29. Luo ML, Zhang WG, Zhang S, Fan J, Su WC, Yin X. Self-assembly and chiral recognition of quartz crystal microbalance chiral sensor. Chirality 2010;22:411–415.
30. Loo JA, Edmonds CG, Smith RD. Tandem mass spectrometry of very large molecules: serum albumin sequence information from multiply charged ions formed by electrospray ionization. Anal Chem 1991;63:2488–2499.
31. Zsila F, Bikádi Z, Simonyi M. Further insight into the molecular basis of carotenoid-albumin interactions: circular dichroism and electronic absorption study on different crocetin-albumin complexes. Tetrahedron: Asymmetry 2002;13:273–283.
32. Zhang YM, Chen Y, Yang Y, Liu P, Liu Y. Supramolecular architectures by fullerene-bridged bis(permethyl-β-cyclodextrin)s with porphyrins. Chem Eur J 2009;15:11333–11340.
33. Liu Y, Li B, Wada T, Inoue Y. Molecular recognition study on a supramolecular system. part 21. inclusion complexation thermodynamics of aliphatic alcohols by organoselenium modified β-cyclodextrins. J Incl Phenom Macrocycl Chem 2000;36:311–325.
34. Guo XJ, Zhang L, Sun XD, Han XW, Guo C, Kang PL. Spectroscopic studies on the interaction between sodium ozagrel and bovine serum albumin. J Mol Struct 2009;928:114–120.
35. Machicote RG, Pacheco ME, Bruzzone L. Binding of several benzodiazepines to bovine serum albumin: fluorescence study. Spectrochim Acta A 2010;77:466–472.
36. Li D, Zhu M, Xu C, Ji B. Characterization of the baicalein-bovine serum albumin complex without or with Cu^{2+} or Fe^{3+} by spectroscopic approaches. Eur J Med Chem 2011;46:588–599.